Journal of Cellular Biochemistry 50:201–209 (1992)

Fluorescence Cytometry of Microtubules and Nuclear DNA During Cell-Cycle and Reverse-Transformation

L. Vergani, P. Gavazzo, P. Facci, A. Diaspro, G. Mascetti, N. Arena, L. Gaspa, and C. Nicolini

Institute of Biophysics, School of Medicine, University of Genoa, Genoa, Italy (L.V., P.G., P.F., A.D., G.M., C.N.) Institute of Histology and Biochemical Technologies, University of Sassari, Sassari, Italy (N.A., L.G.)

Abstract Synchronized CHO-K1 cells and their dibutyryl c-AMP treated counterparts have been characterized by means of static and flow fluorescence cytometry at the level of nuclear DNA and cytoplasmic microtubules.

In order to confirm earlier findings on synchronized population, Carnoy fixed and hydrolyzed, several new findings are here reported at the level of single intact cell. The fluorescence intensity of DAPI-stained glutaraldehyde fixed 2C cells correlates well with the average absorbance of the corresponding Feulgen-stained cells, thereby appearing also to be a measure of chromatin condensation during the G1 phase.

In the early part of G1, the drastic alteration in anti-β tubulin immunostaining is shown to parallel microtubule depolymerization induced by calcium or colcemide.

The known 1–2 h lengthening of the G1 period after reverse-transformation appears to correlate with a similar delay in the abrupt chromatin decondensation.

The above results are discussed in terms of the role of microtubules and nuclear morphometry (and their coupling) in the control of cell cycle progression of transformed vs. fibroblast-like cells.

Key words: immunofluorescence staining, DAPI, microtubules, chromatin, digital image processing, cell morphometry

It is now accepted that the microtubules and the chromatin-DNA structure have impact on various biological processes such as the control of gene expression, protein synthesis, cell cycle regulation, and cell transformation [Brinkley et al., 1975; Brinkley, 1982; Nicolini and Beltrame, 1982; Schliwa, 1986; Leavitt et al., 1987]. Our interest is addressed to further explore the role of the microtubules and nuclear morphometry in the control of normal and abnormal cell growth [Nicolini and Beltrame, 1982; Schliwa, 1986; Leavitt et al., 1987; Belmont et al., 1980], keeping in mind that nuclear morphometry in turn has been shown to be related to the three-dimensional organization of chromatin-DNA and, hence, to gene expression [Belmont and Nicolini, 1983; Kendall et al., 1980; Nicolini, 1986].

We have thereby analyzed CHO-K1 cells and their c-AMP treated counterparts as a function of the cell cycle. Administration of c-AMP to proliferating cells causes a shift from polygonal (called transformed) to a spindle-shaped morphology (called fibroblast-like or reverse transformed) accompanied by a significant change in growth characteristics [Hsie and Puck, 1971; Parodi et al., 1979]. Following earlier studies, which employed harsh Feulgen and Naphtol-yellow absorbance staining, we carried out quantitative fluorescence microscopy (using anti-β tubulin antibodies and DAPI staining) at the level of single fixed cell; flow cytometry was also performed on a larger number of cells properly synchronized for a more statistically significant characterization.

MATERIAL AND METHODS

Cell Culture

In this study we used Chinese hamster ovary fibroblasts (CHO clone K1 supplied by American Type Culture Collection, Rockville, MD) before and after reverse transformation by dibutyryl c-AMP. CHO-K1 cells were routinely grown in F12 medium supplemented with 10% fetal calf serum (Boheringer Mannheim, Sandhofer, FRG); CHO-K1 doubling time was approximately 13 h. Treatment of cells with 10^{-3} M Dibutyryl cyclic 3′,5′ monophosphate adenosine sodium salt (Sigma Chemical Co., St. Louis,

Received June 11, 1992; accepted June 25, 1992.

Address reprint requests to Claudio Nicolini, Institute of Biophysics, School of Medicine, University of Genoa, Genoa, Italy.

MO) induces a drastic change in the cellular shape from polygonal to elongated morphology [Hsie and Puck, 1971]. The effects of c-AMP are probably due to its suboptimal level in transformed cells [Brinkley et al., 1975].

In the treated cells, dibutyryl c-AMP was present from the moment of seeding even in the starting flasks and throughout the entire experimental interval. Treated cells show an elongation of cell cycle duration in agreement with previous observations [Belmont and Nicolini, 1983].

Our experiments were performed on synchronized cells at different times of the cell cycle, namely at 30 min, 1 h, 2, 3, and 6 h after the selective detachment of mitotic cells. This method yields cells optimally synchronized in M, G1, and early S phase, as apparent by the combined utilization of labeling index, Feulgen staining, and optical microscopy [Belmont and Nicolini, 1983; Kendall et al., 1980; Nicolini, 1986; Hsie and Puck, 1971; Parodi et al., 1979]. Mitotic cells were obtained by colcemide block (0.1 μg/ml for 15 h) and early S phase by hydroxyurea (2 mM for 15 h). In order to study the effect of the microtubule depolymerization on the β-tubulin antibody binding cells have been treated either with colcemide (as described above) or with calcium. In the last case CHO-K1 cells synchronized in G1/S phase with hydroxyurea have been treated with 2 mM calcium for 30 min before fixation.

Static Cytofluorimetry

All cells were cultured in petri dishes on sterile coverslips at 37°C, and then fixed in PBS (phosphate buffer saline) containing 0.75% paraformaldehyde, 1.75% glutaraldehyde, 2 mM EGTA, and 2 mM $MgCl_2$ for 1 h at room temperature.

Microtubule staining was accomplished by washing fixed cells in sterile PBS (3 times for 5 min each), then placing in 1% TRITON X100 for 5 min and washing in PBS. Coverslips were placed upside down on microscope slides, previously covered with PARAFILM on which one drop of the first antibody (anti-β tubulin supplied by Biomakor, Rehovot, Israel) was previously placed (to obtain a homogeneous distribution of antibody on the coverslip surface).

In order to prevent evaporation, slides were placed in a moist chamber and incubated at 4°C overnight. After usual washing in PBS, coverslips were incubated with the second antibody (anti-mouse IgG FITC-conjugated, supplied by Sera-Lab, Sussex, England) in the moist chamber at 37°C for 1 h [Tilloca et al., 1987]. Immediately prior to observation, DNA staining was accomplished by 10 μl of 15 μM DAPI (4',6-diamidino-2-phenylindole, supplied by Molecular Probes, Eugene, OR) in 10 mM Tris-HCl buffer, pH 7.2 [Tilloca et al., 1987; Boschek et al., 1981].

Fluorescence dependent images have been acquired through a 100× 1.3 NA oil-immersion objective on a Zeiss Axioplan microscope (Zeiss, Oberoken, FRG) set up for epifluorescence (HBO 100 Osram Mercury Lamp, Zeiss Filter sets 487402, 487709, 487715). Neutral density filters (Kodak, Wratten N.96) have been used to avoid saturation effects on the TV target due to different fluorescence intensities emitted depending on the marker. Calibrations for intensity filters and for geometric corrections have been performed using 10 μm diameter fluoresbrite carboxilate microspheres (Polysciences Inc., Philadelphia, PA).

Flow Cytofluorimetry

Samples for the flow cytofluorimetry were prepared as above but all the steps were performed with cells in suspension and DNA staining was accomplished by a 30 min incubation of the sample in 20 μg/ml propidium iodide and 20 μg/ml RNase in PBS. The samples were analyzed by means of a PAS II flow-microfluorimeter (Partec, Bottmingen, Switzerland) performing two parameter acquisition (PI and FITC). The optical setup was composed of a HBO 100 arc lamp, excitation filters (KG1, BG38), 40× objective, beam splitters (TK 500,630 or 560), mirrors, and filter RG610, OG505 (T). Two parameter data were acquired and processed with the help of modified Assembly software. Calibrations for intensity filters were performed using 480 μm diameter fluoresbrite carboxilate microspheres (Polysciences Inc., Philadelphia, PA) and calf thymocytes.

Digital Imaging

Images directly formed through the optical microscope were computer processed by an integrated image processing system developed in house and previously described in detail [Diaspro et al., 1990a,b,c]. After background subtraction, an intensity threshold was established to define the border of cells and nuclei. This allowed us to calculate cellular and nuclear area. In this context, the term *area* refers to the area of bidimensional projection of the observed ob-

ject. As previously reported [Belmont et al., 1980, 1984; Kendall et al., 1980], for our method of slide preparation, there is a direct correlation between bidimensional projection and both the nuclear volume and the intranuclear DNA distribution.

RESULTS

In Figure 1 the typical frequency distribution of pixel fluorescence intensity is represented for both cells stained with anti-β tubulin antibody (FITC fluorescence) and nuclei stained with DAPI. It doesn't escape our notice that while the intracytoplasmic microtubules display rather uniform unimodal distribution (see Fig. 1A), the intranuclear DNA displays a broad (bimodal) distribution (Fig. 1B) reflecting the existence of different high order structural levels for the nuclear chromatin in G1 phase.

The dependence of DAPI fluorescence intensity on cell cycle progression is presented in Figure 2, both for untreated and c-AMP treated cells. Similar changes of fluorescence intensity are exhibited by the two populations: both dis-

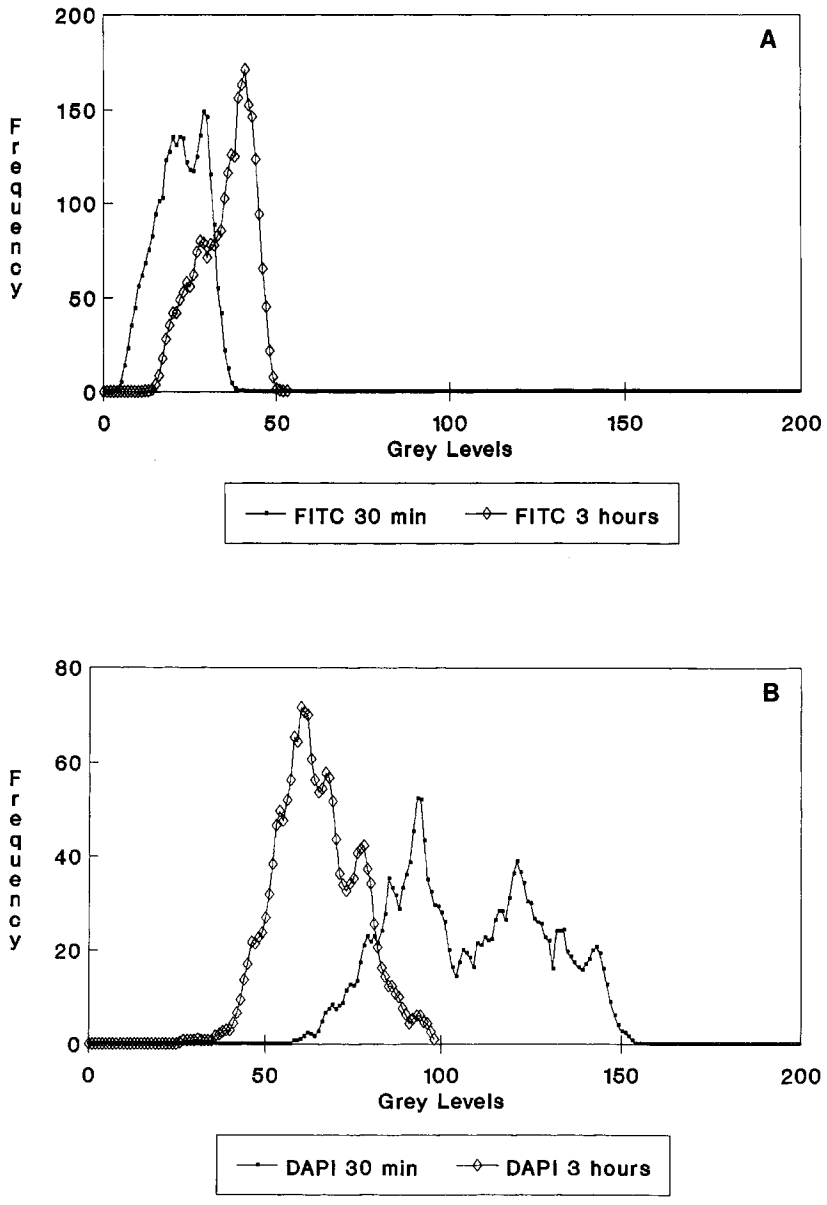

Fig. 1. Histograms representing the number of pixel vs. fluorescence intensity obtained from two typical images of synchronized CHO-K1 cells at 30 min and 3 h after mitosis and simultaneously stained (**A**) for microtubules with anti-β tubulin antibodies FITC conjugated and (**B**) for nuclear DNA with DAPI.

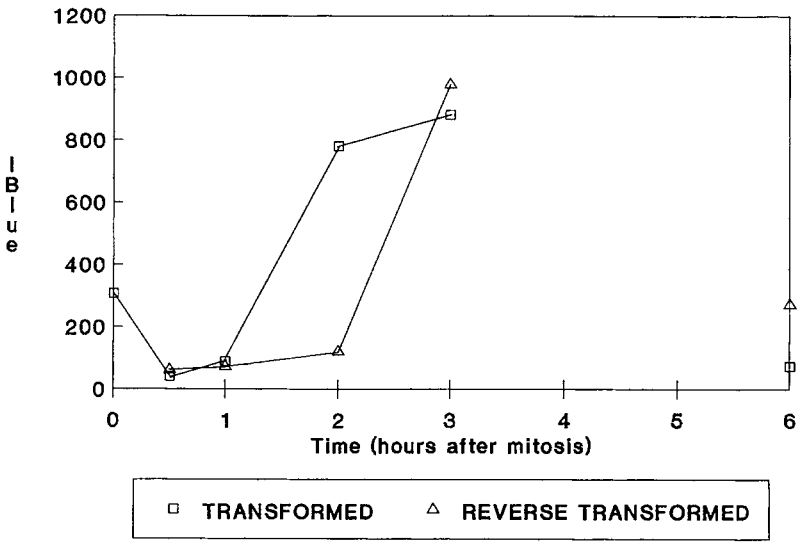

Fig. 2. Blue fluorescence intensity (IBLUE) vs. time for untreated (□) and c-AMP treated (△) CHO nuclei, stained with DAPI.

play an initial decrease of fluorescence intensity at 30 min (early G1) followed by an increase during the next 3 h (G1 period) and subsequently by another decrease at 6 h (late G1/early S phase). This is apparent even after normalizing for the DNA amount (4C in mitosis and 2C in G1). The most abrupt increase is between 1 and 2 h for untreated CHO and between 2 and 3 h for c-AMP treated ones, in accordance with the known 1–2 h lengthening of G1 period after cAMP administration.

The direct correlation between DAPI fluorescence intensity (IBLUE) and nuclear area for untreated control cells having the same 2C amount of DNA is shown in Figure 3A; both cell populations exhibit a very good correlation between these two parameters ($P < 0.01$ both for untreated and c-AMP treated CHO). In the same figure, the reverse correlation between average optical density (AVOD) and nuclear area is also represented for the same 2C DNA cell population stained by Feulgen reaction; the amount of DNA per cell remains constant in this population, as shown by the constant value of the integrated optical density (IOD) (data not shown).

The established correlation between AVOD and chromatin condensation suggests a possible interpretation of the staining characteristics of DAPI, whereby the binding of DAPI to the nuclear DNA could appear a direct function of chromatin decondensation.

The lack of correlation between cytoplasmic anti-β tubulin fluorescence (IGREEN) and cell area is reported in Figure 3B; namely β-tubulin immunostaining shows a constant value, between 1 and 6 h after mitosis, for a wide range of cell areas.

Confirming earlier data [Belmont et al., 1984], during cell cycle progression the correlation between cellular and nuclear area (Fig. 4) appears, at the 1% confidence level, good for the fibroblast-like cells ($r = 0.80$) and lacking for the untreated ones ($r = 0.57$; figure not shown). However, no difference of FITC intensity is evident for the two cell types: during the cell cycle both display indeed the same behavior in anti-β tubulin staining (Fig. 5).

The maximum of FITC fluorescence is evident, for both samples, 30 min after mitosis when the cells go through the depolymerization of mitotic spindle and reorganization of cytoskeleton. During the rest of the cell cycle the IGREEN values remain nearly constant.

The flow cytometry of over 65,000 cells double stained both for microtubule (with FITC) and chromatin-DNA (with propidium iodide) confirms the increase of the cytoplasmic IGREEN of the colcemide-treated cells in respect to the untreated ones (Fig. 6). The abrupt decrease in immunofluorescence staining from mitosis to early G1 could be related to the tubulin polymerization which causes a decreased binding of the antibodies; an opposite effect is indeed apparent whenever microtubule depolimerization is achieved by 2 mM calcium administration to hydroxyurea synchronized cells (Fig. 7). For the

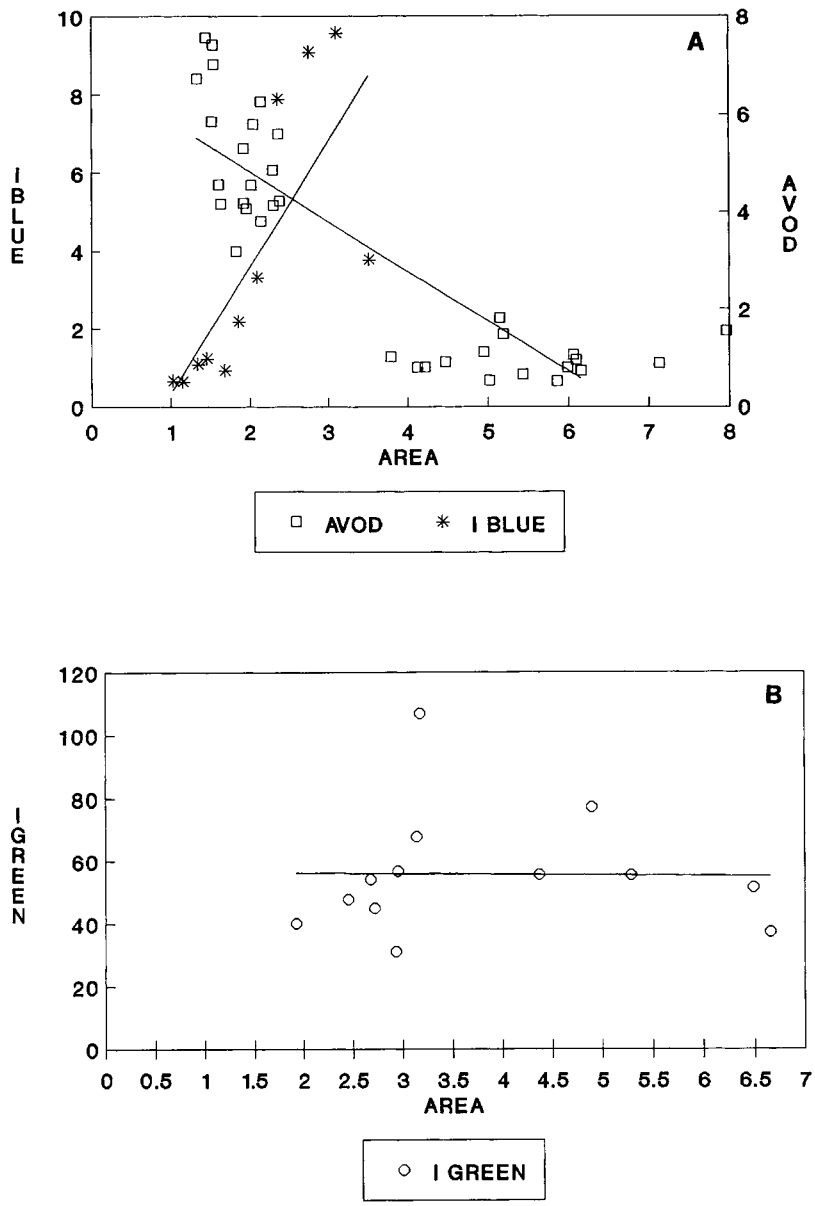

Fig. 3. **A:** Correlation between nuclear total fluorescence intensity (IBLUE) and area for untreated CHO; the value of correlation coefficient is 0.75 (at the confidence level less than of 1%). The correlation between average optical density determined by Feulgen staining and area is also shown for the same nuclei (□). **B:** Correlation between cellular IGREEN and area for c-AMP treated CHO cells.

same sample the corresponding average values of IGREEN and area are shown in Table II.

DISCUSSION

The presented data, which are based on a fluorescence staining of gluteraldheide fixed cells, confirm earlier results based on absorbance staining of the corresponding Carnoy fixed and hydrolyzed cells [Nicolini and Beltrame, 1982; Schliwa, 1986; Leavitt et al., 1987; Belmont et al., 1980]: the correlation between cellular and nuclear geometry is present in c-AMP treated cells but is absent in the untreated cells. Similarly the existence of two cycles of chromatin condensation during the G1 period of both c-AMP treated and untreated cells appears confirmed, while the increase of G1 period by 1–2 h following c-AMP administration (as originally suggested by previous reports [Parodi et al., 1979; Belmont et al., 1984; Nicolini et al., 1987])

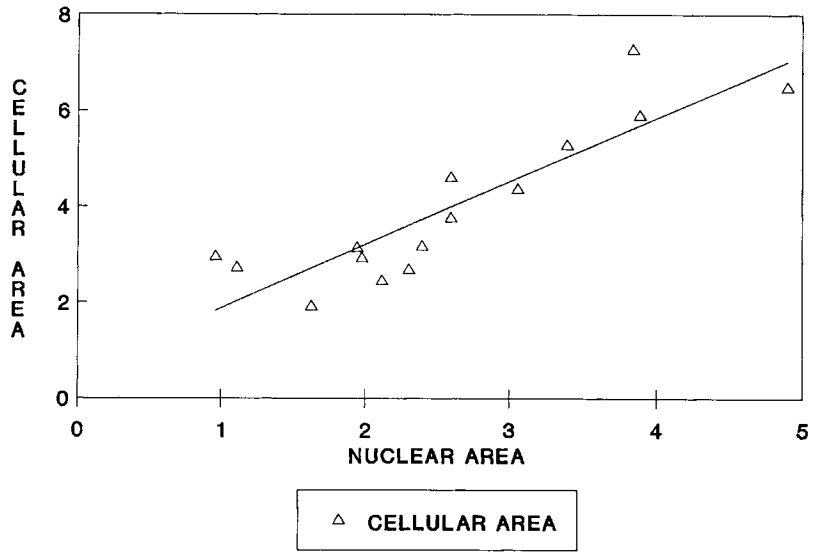

Fig. 4. Correlation between cellular and nuclear area for fibroblast-like CHO, synchronized at 0, 0.5, 1, 2, 3, and 6 h after mitosis.

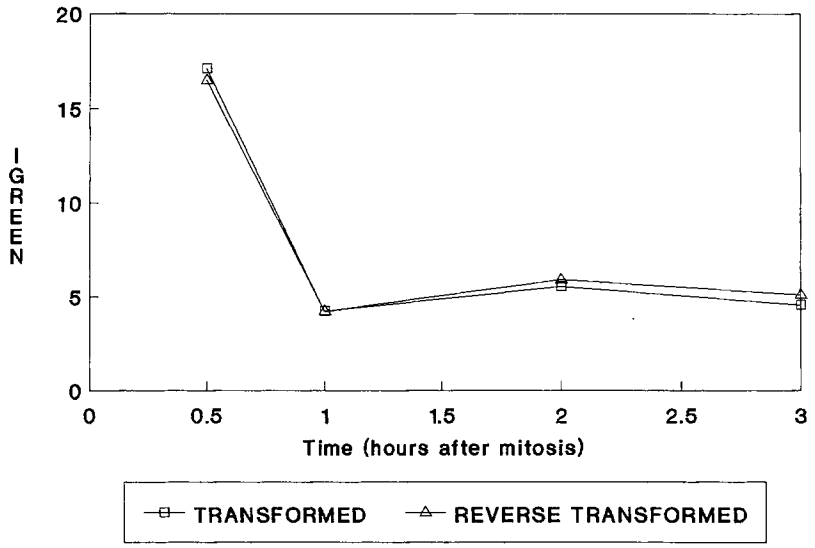

Fig. 5. Green fluorescence intensity (IGREEN) vs. time both for untreated (□) and c-AMP treated (△) CHO cells stained by immunofluorescence technique with anti-β tubulin antibodies. The standard deviations are about 40% for the untreated and 45% for the c-AMP treated nuclei.

appears correlated with a similar delay in chromatin decondensation. This new observation supports earlier suggestions on the role of chromatin-DNA in the control of DNA replication.

Additional conclusions can be drawn from the above data. The use of anti-β tubulin monoclonal antibodies makes it possible to correlate the difference of cytoplasmic fluorescence intensity with the level of microtubule polimerization. This correlation is confirmed by the higher level of immunofluorescence in cells treated with different depolymerizing agents (colcemide and calcium) in respect to control cells.

The results of quantitative fluorescence microscopy show significant changes during the cell cycle progression: the decreased immunofluorescence in the early part of G1 appears to be only partially due to the distribution caused by cell division, but is related to a larger extent to the microtubule polymerization which could

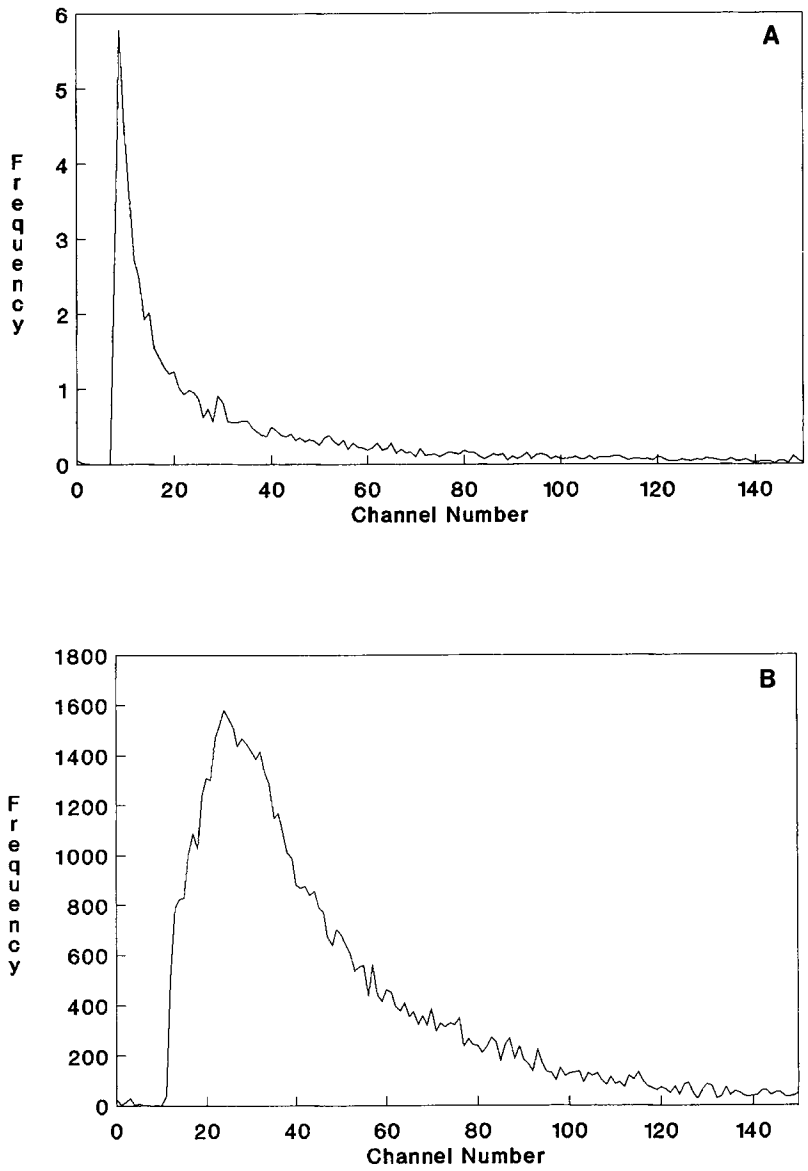

Fig. 6. Fluorescence intensity histograms for CHO-K1, either synchronized in mitosis with colcemide to depolymerize the cytoskeleton (A) or logarithmically grown (B). The cells have been immunostained for anti-β tubulin as described in the text.

make tubulin less accessible to the monoclonal antibodies. This microtubule polimerization observed 1 h after mitosis is associated with an increase in nuclear area (Fig. 2) which perfectly matches with the restoration of metabolic activity of the cell.

A drastic increase in tubulin synthesis in G2 just before mitosis, followed by a similarly drastic decrease at the end of mitosis, when the cells enter the G1 phase, was reported previously. These facts were actually used to develop a model which implies that elevated levels of soluble tubulin inhibit new tubulin mRNA synthesis [Klevecz and Forrest, 1975; Bird et al., 1980].

No significant difference in the total intensity of anti-β tubulin immunostaining were detected for the untreated and the c-AMP treated cells, in agreement with previous biochemical studies. These data combined with earlier observations [Brinkley, 1982; Hsie and Puck, 1971] led us to postulate that untreated and c-AMP treated cells differ only in terms of microtubule three-dimensional organization and orientation and are quite similar in terms of the amount of polymerized

Fig. 7. CHO-K1 cells synchronized in G1/S phase by hydroxyurea before (left) and after treatment (right) with 2 mM $CaCl_2$ for 30 min. Cells are stained with anti-β tubulin antibodies. Image has been filtered with a Gaussian Low-Pass to reduce the spatial-distributed noise present in the original image and then a histogram-equalization operation has been applied to improve details in the image.

TABLE I. CHO-K1 Cells Synchronized in Early S Phase (by hydroxyurea 2 mM) and in Mitosis (by colcemide 0.1 μg/ml)*

		Mitosis (M)		Early S (eS)	
		μ	σ (%)	μ	σ (%)
	IOD	962	21	534	47
Feulgen	Area	1,884	17	5,467	20
	AVOD	0.52	24	0.10	37
DAPI	IBLUE	168,328	53	201,024	38
	Area	2,140	32	5,156	16

Relative Increase in Chromatin Decondensation Between Mitosis and Early S as Measurement by Feulgen Absorbance and DAPI Fluorescence Intensity After Normalization to the Same Amount of 2C DNA

Feulgen	$\frac{AVOD_M}{AVOD_{eS}}$	5.2
DAPI	$\frac{2xIBLUES_{eS}}{IBLUE_M}$	2.2

*The samples have been stained from one side by Feulgen reaction and and from the other side by DAPI.
AVOD = average optical density; IBLUE = total fluorescence intensity; IOD = integrated optical density.

TABLE II. CHO-K1 Cells Synchronized at the G1/S Interphase by 2 mM Hydroxyurea Before (control) and After the Treatment With 2mM $CaCl_2$

Sample	FITC fluorescence intensity (IGREEN)	Area
Control	μ = 165,213 σ = 24%	μ = 4,138 σ = 7%
Calcium treated	μ = 201,242 σ = 25%	μ = 5,398 σ = 5%

tubulin. Hence, it appears that either a higher level of microtubule organization or other components of cytoskeleton are responsible for the observed correlation between cellular and nuclear area.

Finally, previous papers [for review see Nicolini, 1986, 1983] have shown that the nuclear area is directly correlated with chromatin-DNA condensation and that IOD and AVOD parameters, evaluated on Feulgen-stained cells, are related to the total DNA amount and the chromatin condensation, respectively.

The inverse linear relationship evident for AVOD (Feulgen-stained) and IBLUE (DAPI staining) is another interesting new observation which deserves some consideration.

It was recently established [Kubista et al., 1987; Kapuscinski, 1990] that DAPI can bind nucleic acid in a double helix conformation with both a mechanism of intercalation between the stacking base pairs and an electrostatic binding to the AT-rich regions present in the minor groove. The second kind of binding has been

known for a long time and shows a quantum yield and an affinity much greater than the first one [Kapuscinski, 1990]. However, it was not clear if and how the fluorescence intensity shown by the dye binding to DNA is related to the level of chromatin condensation. Our results in Table I and Figure 3 suggest that binding of DAPI to DNA is really affected by the level of chromatin condensation.

ACKNOWLEDGMENTS

We would like to thank Paolo Milani, Eugenia Rivano, and Stefania Urbini for their technical support, Manuela Adami and Marco Sartore for their collaboration, Maria Raffaele and Sergey Vakula for their linguistic assistance, and Sonia Zara for her typing the manuscript. This work has been supported by CNR 89.00191.70 and 89.02845.04 and MURST M.P.I. 40%. L.V., P.G., and G.M. are supported by MURST a fellowship.

REFERENCES

Belmont AS, Kendall FM, Nicolini CA (1980): Coupling of nuclear morphometry to cell geometry and growth in human fibroblast. Cell Biophysics 2:165–175.

Belmont AS, Kendall F, Nicolini C (1984): Three dimensional intranuclear DNA organization in situ: Three states of condensation and their redistribution as a function of nuclear size near the G1-S borderin HeLa S3 cells. J Cell Science 65:123–138.

Belmont AS, Nicolini CA (1983): The G1 period two cycle of chromatin conformational changes monitored by single cell dye intercalation. Cell Biophysics 5:79–94.

Bird RC, Zimmerman S, Zimmerman A (1980): Tubulin synthesis during the cell cycle. In "Nuclear Cytoplasmatic Interactions in the Cell Cycle. NewYork: Academic Press, Inc., pp 350–360.

Boschek CB, Jockusch BM, Friis RR, Back R, Grundmann E, Bauer H (1981): Early changes in the distribution and organization of microfilament proteins during cell transformation. Cell 24:175.

Brinkley BR, (1982): The cytoskeleton: An intermediate in the expression of the transformed phenotype in malignant cells. In Nicolini C (ed): "Chemical Carcinogenesis." New York: Plenum Press, pp 435–467.

Brinkley BR, Fuller GM, Highfield DP (1975): Cytoplasmic microtubules in normal and transformed cells in culture: Analysis by tubulin antibody immunofluorescence. Proc. Natl. Acad. Sci. USA 72:4981–4985.

Diaspro A, Adami M, Nicolini C (1990c): Three-dimensional representation of biostructures imaged with an optical microscope. II. Graphic 3D representation. Image and Vision Computing 8:134.

Diaspro A, Adami M, Sartore M, Nicolini C (1990a): IMAGO a complete system for acquisition, processing and 2D/3D and temporal display of microscopic bioimages. Computer Methods and Programs in Biomedicine 31:225.

Diaspro A, Sartore M, Nicolini C (1990b): Three-dimensional representation of biostructures imaged with an optical microscope. I. digital optical sectioning. Image and Vision Computing 8:130.

Hsie AW, Puck TT (1971): Morphological transformation of Chinese hamster cells by dibutyryl-adenosine cyclic 3′:5′ monophosphate and testosterone on mammalian cells. Proc Natl Acad Sci USA 68:358.

Kapuscinski J (1990): Interaction of nucleic acids and fluorescent dyes. J Histochem Cytochem 38:1323.

Kendall FM, Beltrame F, Zietz S, Belmont A, Nicolini CA (1980): The quinternary chromatin-DNA structure. 3D reconstruction and functional significants. Cell Biophysics 2:373–404.

Klevecz RR, Forrest GL (1975): Ann N Y Acad Sci 253:292.

Kubista M, Akerman B, Norden B (1987): Characterization of interaction between DAPI and DNA by optical spectroscopy. Biochemistry 26:4545.

Leavitt J, Sun YN, Madmu V, Latter G, Burbek S, Gunning P, Kedes L (1987): Expression of transformed mutant β-actin genes: Transition toward the stable tumorigenic state. 7:2467–2476.

Nicolini C (1983): The high order structure of chromatin-DNA: From nuclei to gene. Anticancer Res 3:63.

Nicolini C (1986): "Biophysics and Cancer." New York: Plenum Press.

Nicolini C, Beltrame F (1982): Coupling of chromatin structure to cell geometry during the cell cycle: Transformed versus reverse-transformed CHO. Cell Biology International Reports 6:1.

Nicolini C, Diaspro A, Vergani L, Bertolotto M, Germano P (1987): Nuclear architeture, intranuclear DNA distribution and nuclease digestion. Cell Biophysics, 13:1–12.

Parodi S, Beltrame F, Lessin S, Nicolini C (1979): Morphometric analysis of B cAMP-induced reverse transformation in synchronized CHO cells. Cell Biophysic 1:271–292.

Schliwa M (1986): "The Cytoskeleton: An Introductory Survey." Wien, New York: Springer-Verlag.

Tilloca G, Pippia P, Sciola L, Meloni MA, Gaspa L, Arena N (1987): Appearance of adhesion plaque proteins in neoplastic cultured cells (SGS/3A) by immunofluorescence. Eur J Cell Biol 44:27.